Supporting Information

Methane Adsorption in Metal-Organic Frameworks Containing Nanographene Linkers: a Computational Study

Elena Bichoutskaia,[*] Mikhail Suyetin, Michelle Bound, Yong Yan and Martin Schröder

School of Chemistry, University of Nottingham, University Park, Nottingham NG7 2RD, UK

A new family of the (3,24)-paddlewheel-connected MOF networks with *rht* topology has been designed, in which hexabenzocoronene molecule has been used to replace the phenyl ring traditionally used as a central element of the linkers in (3,24)-paddlewheel-connected MOFs. The structures of the model MOFs family are shown in Figure S1.
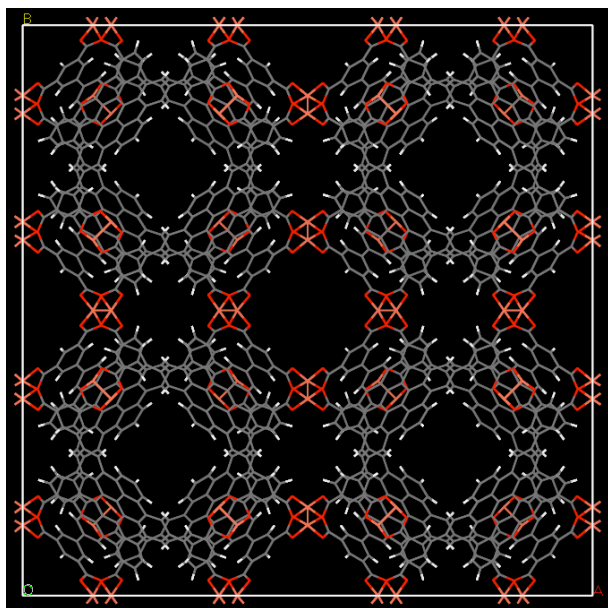
MOF-L[0]
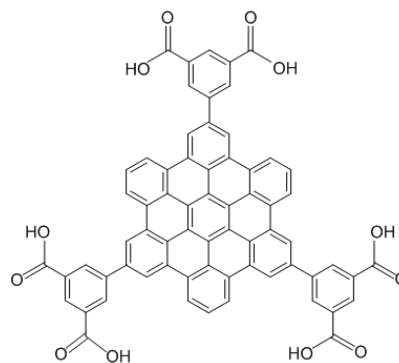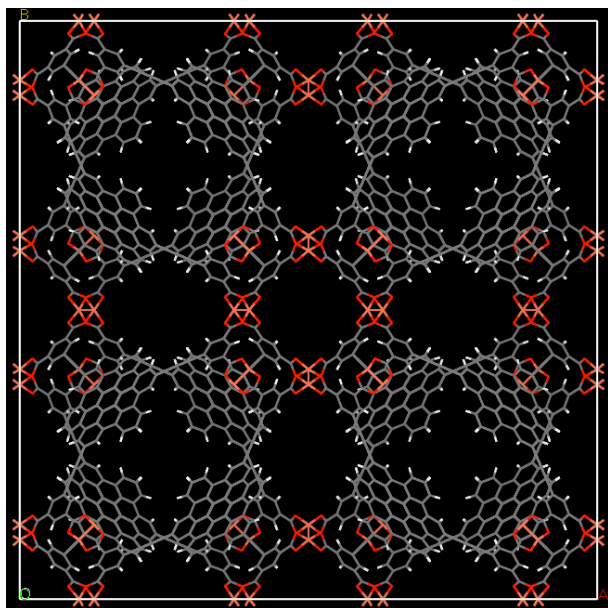
MOF-L^1
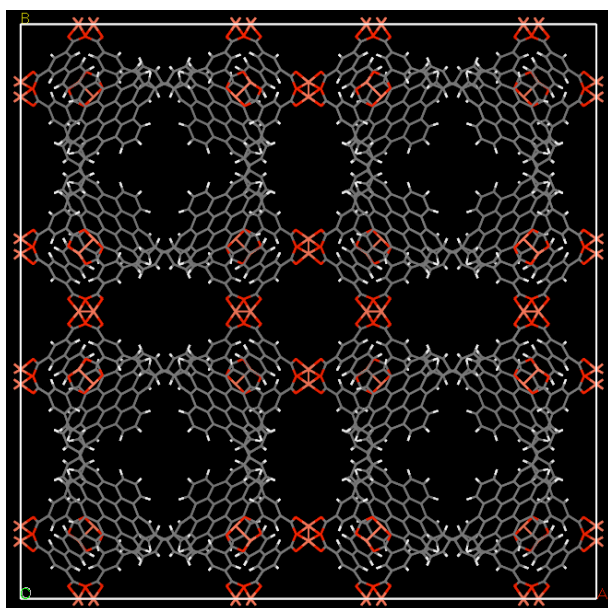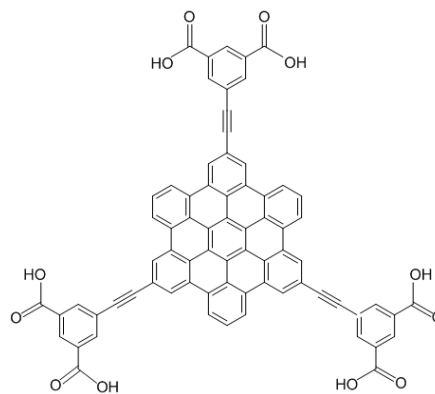
MOF-L^2
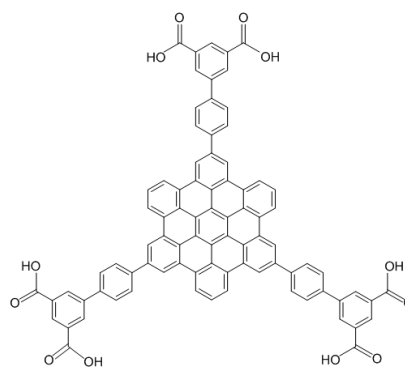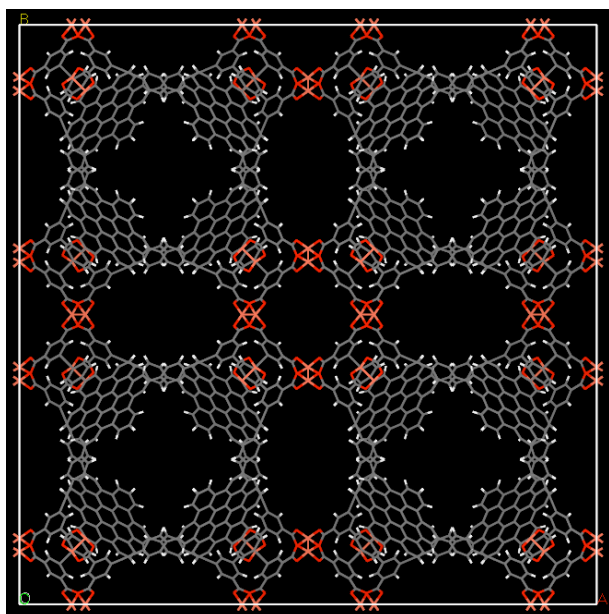
MOF-L³
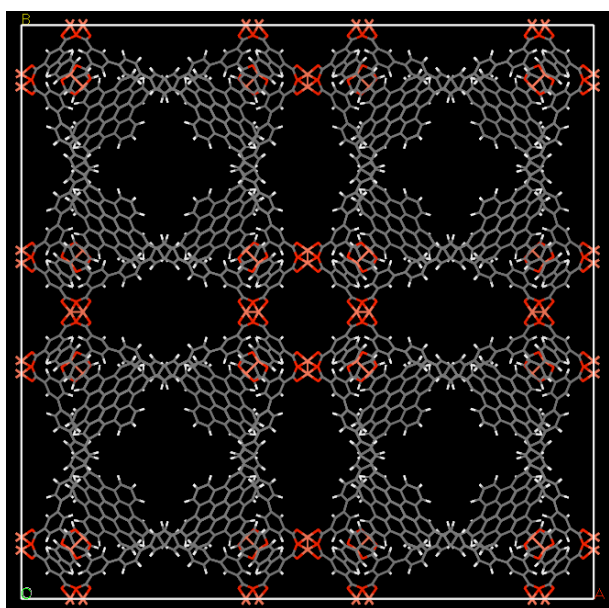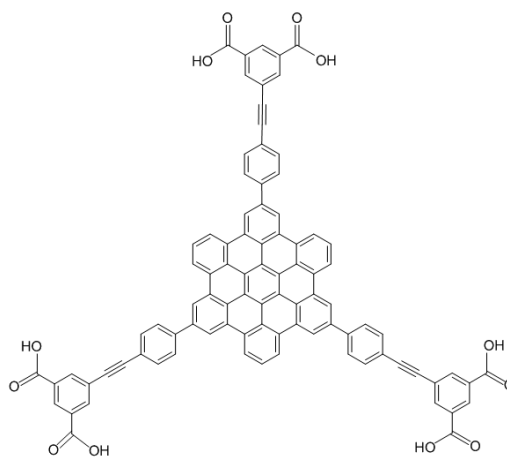
MOF-L⁴
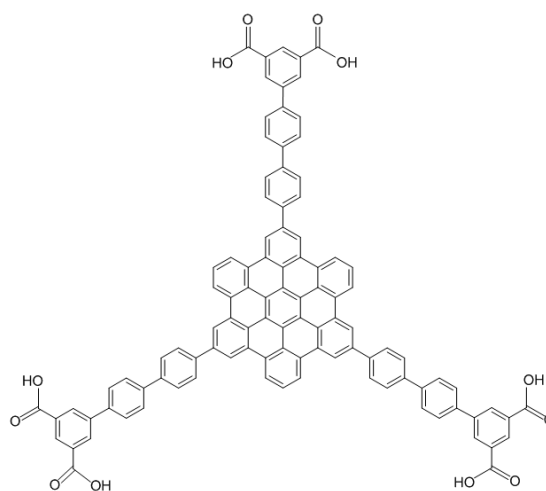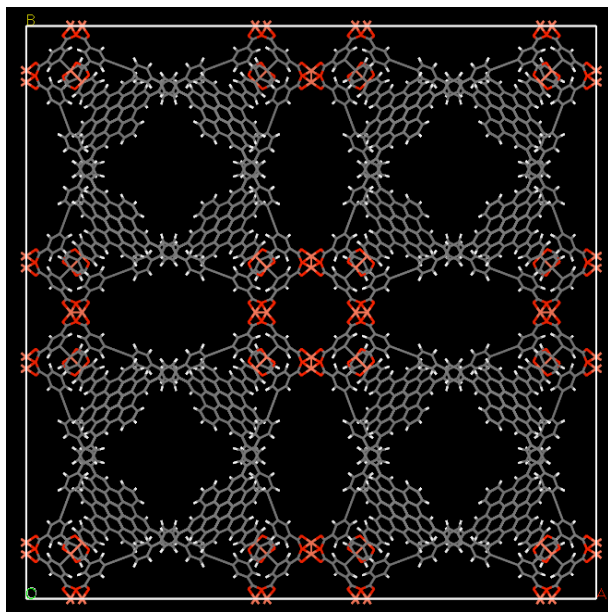
MOF-L⁵
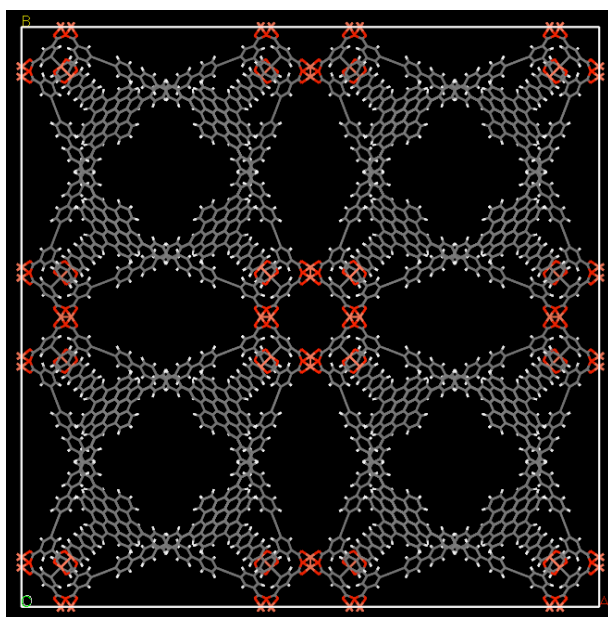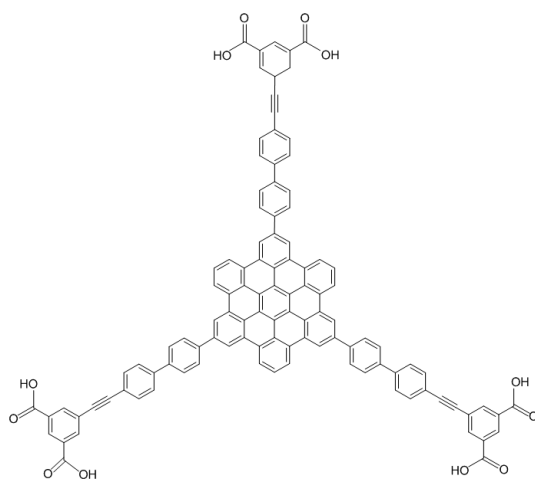
MOF-L⁶
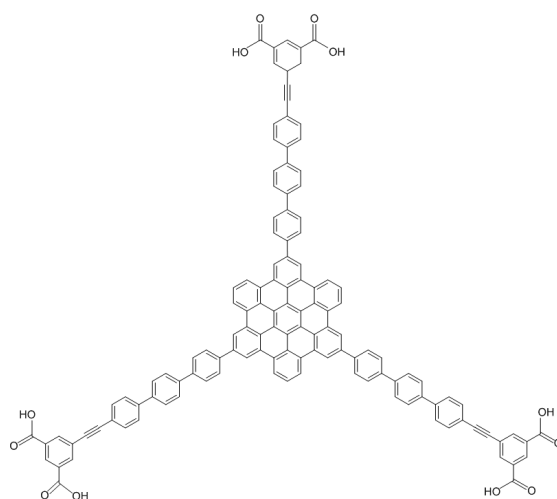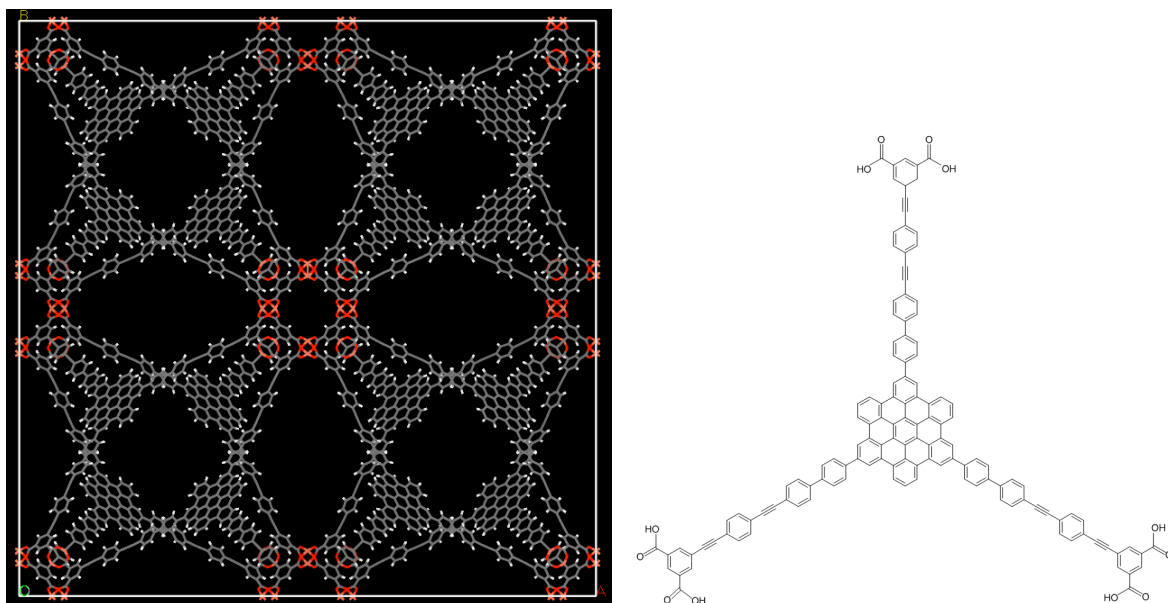
MOF-L[7]

Figure S1: A series of MOFs with a central linker part comprising hexabenzocoronene unit.

The new series exhibit the increased surface area and pore volume. This is illustrated in Figure S2 where the dimensions of a series of experimentally obtained MOF linkers and their modification with hexabenzocoronene have been compared.

12.23 Å	18.97 Å
L(PCN-61)	**L[1]**
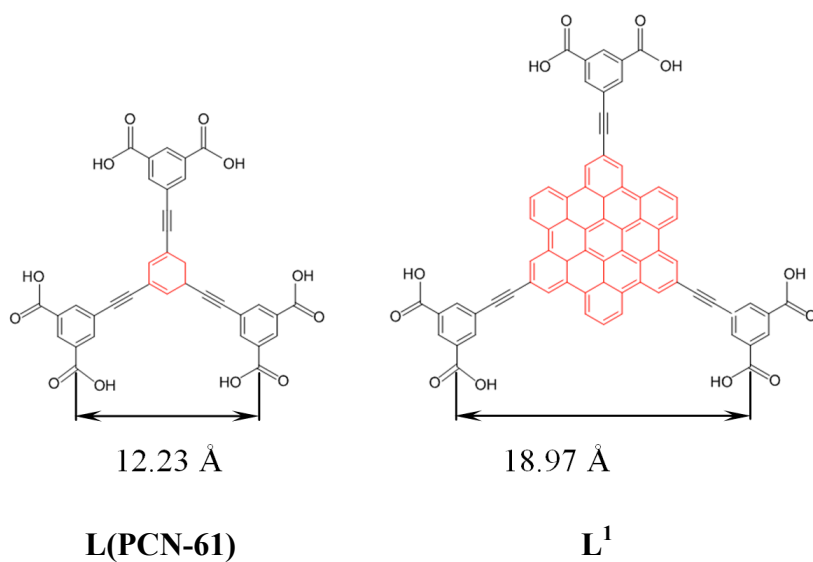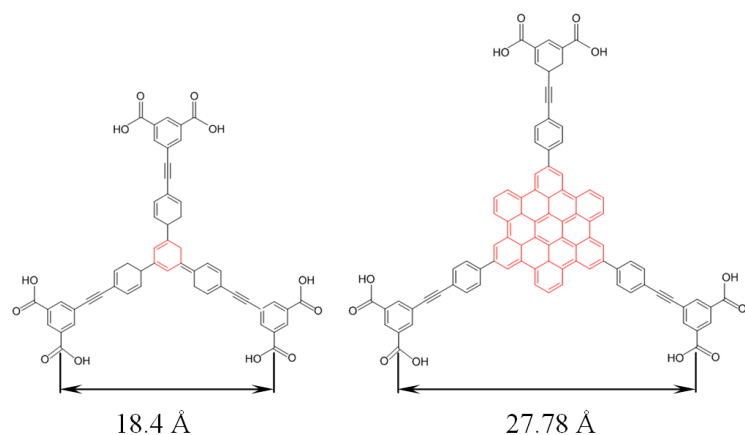
NOTT-116/PCN-68   **L^3**
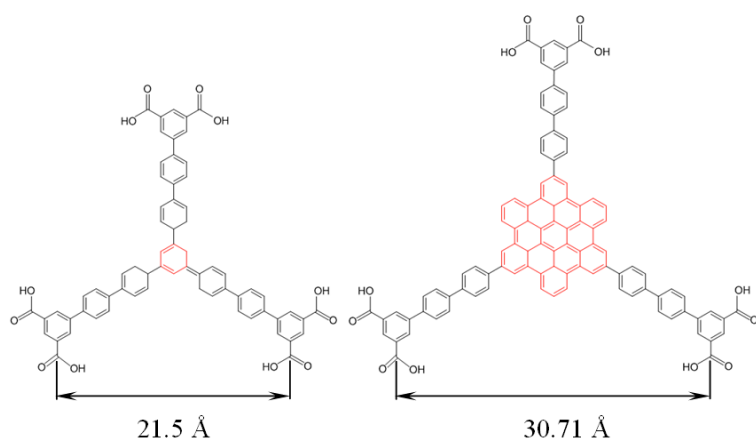
L(NOTT-119/PCN-69)   **L^4**

Figure S2: Linkers of MOFs obtained by modification with hexabenzocoronene and linkers of experimental MOFs.

Structure optimization

NOTT-112 was chosen a starting point for structure preparation of the series of MOFs studied in this work. The *rht*-network topology, copper paddlewheel cluster and group symmetry of *Fm3m* were maintained. The series of MOFs were built, and geometry optimization of the structures undertaken using molecular mechanics simulations. These calculations were performed with the Forcite module of Materials Studio.[1] Universal Force Field (UFF) parameters[2] were used for the bonded and non-bonded interactions, with the exception of electrostatic interactions for which the Ewald sum technique was employed. Partial atomic charges were calculated using charge equilibration approach[3] developed by Goddard for use in molecular dynamics simulations. During geometry optimisation the convergence criteria for the maximum change in the length of the unit cell is 0.01 Å.

A slightly different approach was used for the largest structure **MOF-L**[7]. Density Functional Theory (DFT) calculations were performed to derive the charges which were then used in the geometry optimization calculation to predict the final structure of **MOF-L**[7]. These were performed on clusters derived from the unit cells and atomic coordinates of **MOF-L**[7], which included metal ion nodes and the organic linker representative of the respective unit cells, as shown in Figure S3. All DFT calculations were performed with the Q-Chem quantum chemistry package[4] at B3LYP level of theory and the 6-31G* basis set. Partial atomic charges were extracted using the ChelpG technique,[5] originally developed by Breneman and Wiberg. The final charge values were used for simulation of H_2 and CO_2 sorption. Details of the partial atomic charges can be found in Table S1. It was noted that through each cycle of optimisations, the differences between partial atomic charges on the atoms within the MOF decreased. This illustrated the structural convergence of the MOF through repeated optimisations. It was also noted that the partial charges on the central hexabenzocoronene part of the linker and also the nodes containing the open Cu(II) sites varied by a very small amount during optimisations. The biggest differences in partial charges were in the areas linking the nodes and central parts of the linker. As will be shown later, this illustrates the structural change that the linker undergoes through the optimisations.
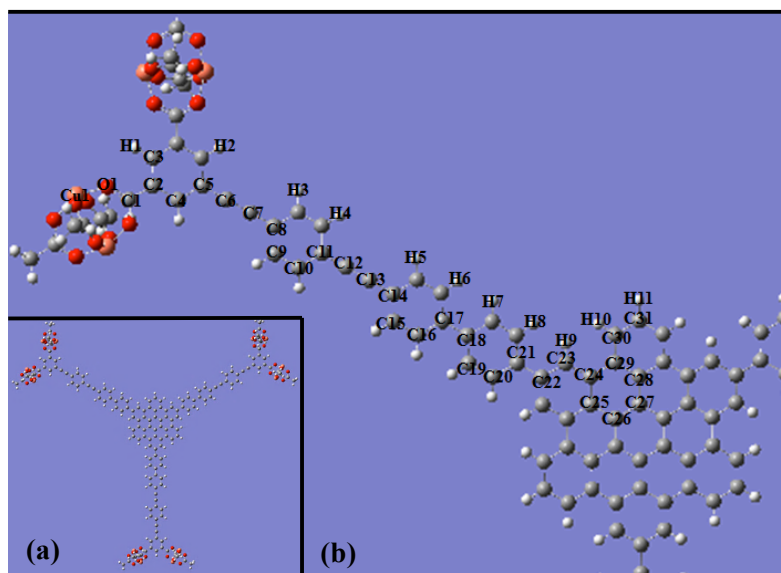
Figure S Error! No text of specified style in document.**3**: View of the cluster used to derive partial charges on the atoms in **MOF-L**[7]; (a) the entire cluster and (b) the linker fragment showing atoms with different environments within the MOF that were assigned partial charges. Red, oxygen; orange, copper; grey, carbon; white, hydrogen.

Table S1: Partial atomic charges for atoms in **MOF-L**[7].

Atom	Cu1	O1	C1	C2	C3
Charge (e)	1.198	-0.672	0.807	-0.137	-0.001
Atom	H1	C4	H2	C5	C6
Charge (e)	0.087	-0.089	0.120	0.165	-0.137
Atom	C7	C8	C9	H3	C10
Charge (e)	-0.153	0.207	-0.163	0.138	-0.184
Atom	H4	C11	C12	C13	C14
Charge (e)	0.140	0.236	-0.158	-0.164	0.241
Atom	C15	H5	C16	H6	C17
Charge (e)	-0.171	0.129	-0.144	0.123	0.058
Atom	C18	C19	C20	H8	C21
Charge (e)	0.066	-0.141	0.115	0.124	0.086
Atom	C22	C23	H9	C24	C25
Charge (e)	0.052	-0.175	0.111	0.013	0.025
Atom	C26	C27	C28	C29	C30
Charge (e)	0.002	-0.031	0.029	0.030	-0.147
Atom	H10	C31	H11		
Charge (e)	0.119	-0.104	0.112		

Gas uptake simulation

Grand Canonical Monte Carlo (GCMC) simulations were performed to calculate the adsorption of gases in the model MOFs. Periodic boundary conditions were applied to a unit cell, and the fugacity was calculated from the Peng-Robinson equation of state.[6] The MOF framework and the gas molecules were considered to be rigid. Lennard-Jones (LJ)

potential was used to describe the Van der Waals interactions with a cut-off distance of 12.8 Å. The GCMC simulations were performed with MUSIC simulation suite[7] and included $2 \cdot 10^7$ step equilibration period followed by $2 \cdot 10^7$ step production run. The LJ parameters for atoms in the MOF and the values used in the simulations are shown in Table S2. Most of the LJ parameters were taken from the DREIDING force field, which uses general force constants and geometric parameters based on simple hybridisation considerations. The copper LJ parameters were taken from the UFF. Previous research has shown that gas adsorption modelled with parameters taken from these force fields have produced reliable results in agreement with experimental work. Partial charges for atoms in the MOF were derived from DFT calculations using the ChelpG approach as described previously and used for simulation of H_2 and CO_2 sorption in **MOF-L**[7] only.

Table S2: LJ parameters for atoms present in MOFs.

Atom type	σ (Å)	ε/k_B (K)
C	3.473	47.856
O	3.033	48.158
H	2.846	7.649
Cu	3.114	2.516

Methane model: The simulation parameters for CH_4 were taken from the TraPPE force field.[8] The CH_4 molecule was represented as a united-atom and the LJ parameters for the methane model are shown in Table S3.

Table S3: LJ parameters for methane.

	σ (Å)	ε/k_B (K)
CH_4	3.73	148.0
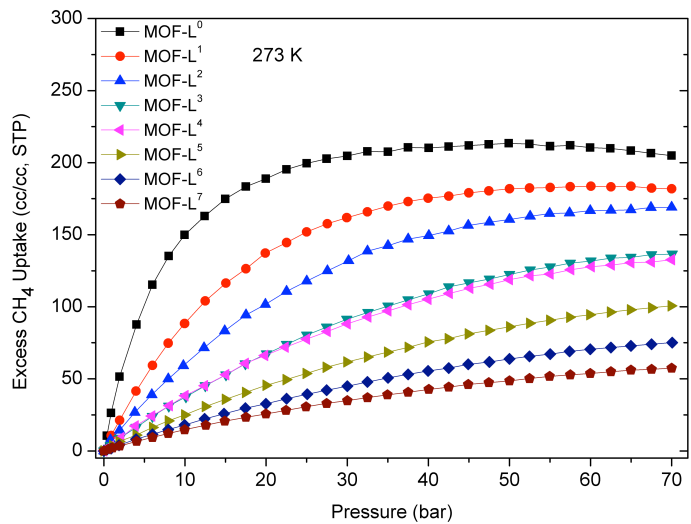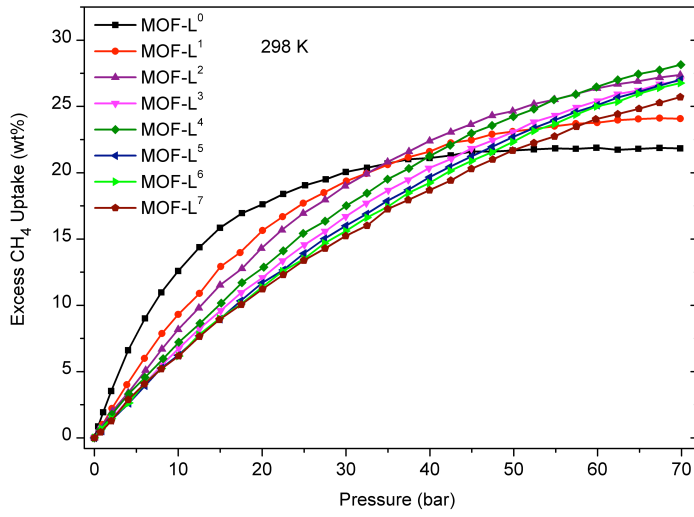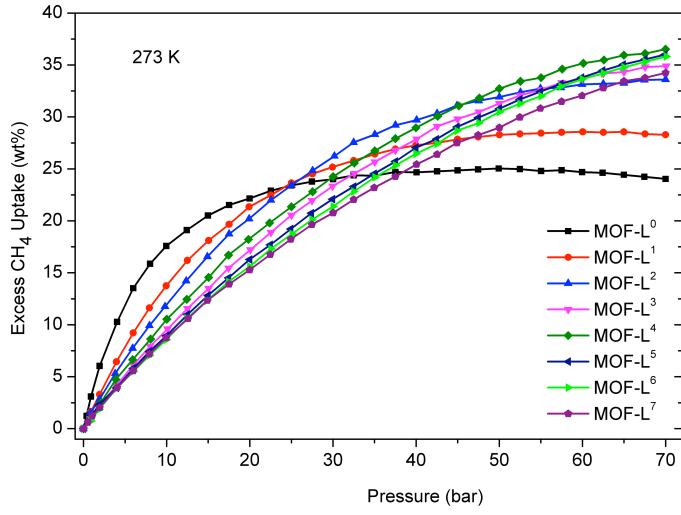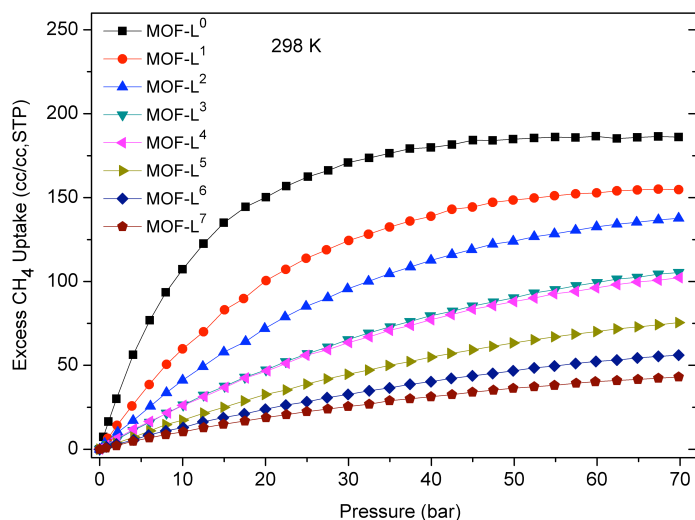
Figure S4. Calculated excess adsorption isotherms for CH_4 in model MOFs with the **L⁰-L⁷** organic linkers at T = 273, 298 K.

Hydrogen model: For H_2 molecules, the Lennard-Jones parameters came from experimental work and the model used was the same as used by Dakrim *et al.*[9] H_2 was modelled as a rigid structure with a set bond length of 0.74 Å and was represented by a single van der Waals sphere. This reproduced the quadrupole moment of a H_2 molecule by placing partial charges on the hydrogen atoms and at the centre of mass. The LJ parameters for the H_2 model along with the partial charges are shown in Table S4.

Table S4: LJ parameters and partial charges for the sites in the hydrogen molecule.

Atom Type	σ (Å)	ε/k_B (K)	q (e)
H	0	0	0.468
H_2 (COM)	2.958	36.7	-0.936

Carbon dioxide model: CO_2 molecules were modelled using the TraPPE force field[10] and was modelled as a rigid structure free to move about the MOF with a fixed C-O bond length of 1.16 Å. CO_2 has a permanent quadrupole moment so was modelled as three van der Waals spheres by placing partial charges on the carbon and both oxygen atoms. The values of the LJ parameters and these partial charges are shown in Table S5.

Table S5: LJ parameters and partial charges for the sites in the carbon dioxide molecule.

Atom Type	σ (Å)	ε/k_B (K)	q (e)
C	2.80	27.0	0.7
O	3.05	79.0	-0.35

Snapshots of CO_2 filling the pores of **MOF-L**[7] at different pressures through the simulation are shown in Figure S5.
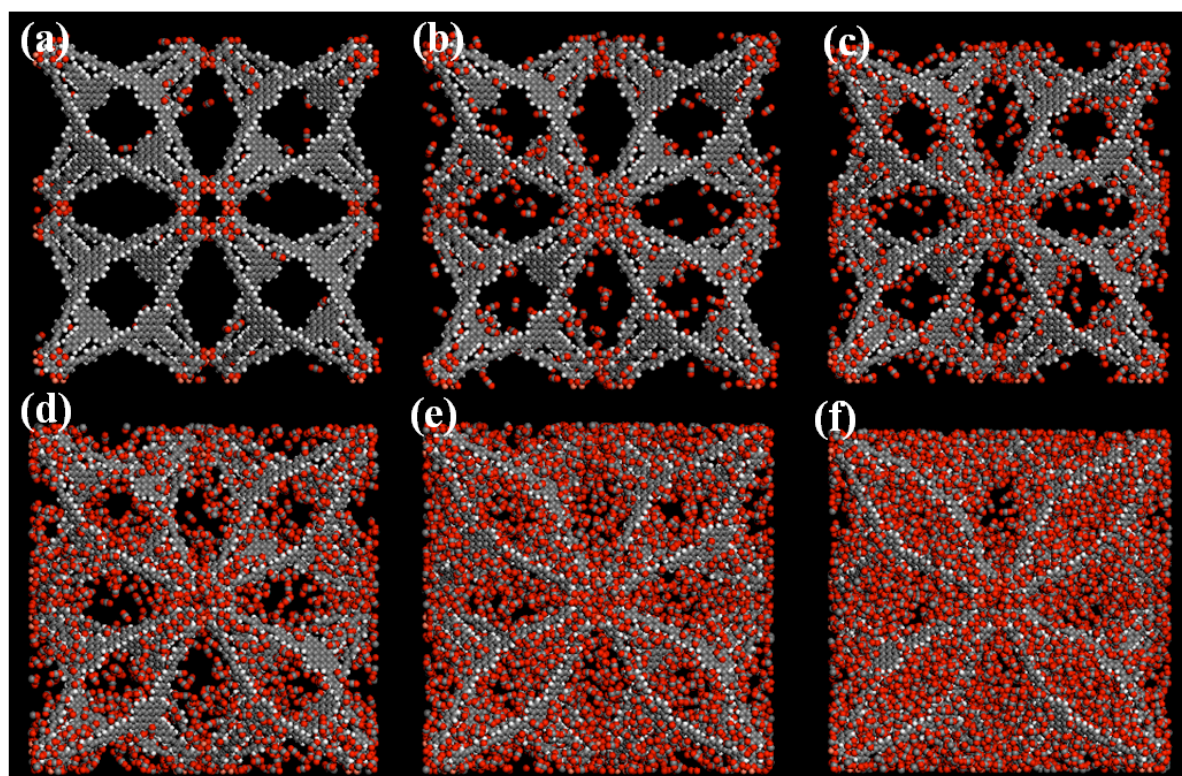
Figure S5: Snapshots of simulated carbon dioxide adsorption within **MOF-L**[7] (298 K); (a) 1 bar, (b) 5 bar, (c) 10 bar, (d) 20 bar, (e) 30 bar and (f) 40 bar. Red, oxygen; orange, copper; grey, carbon; white, hydrogen.

References:

1. Materials Studio 5.0, Accelrys Software Inc., San Diego, CA 92121, USA

2. Rappe, A. K.; Casewit, C. J.; Colwell, K. S.; Goddard III, W. A.; Skid, W. M. *J. Am. Chem. Soc.* **1992**, *114*, 10024−10035.

3. Rappe, A. K.; Goddard III, W. A. *J. Phys. Chem.* **1991**, *95*, 3358−3363.

4. Shao, Y.; Molnar, L. F.; Jung, Y.; Kussmann, J.; Ochsenfeld, C.; Brown, S. T.; Gilbert, A. T. B.; Slipchenko, L. V.; Levchenko, S. V.; O'Neill, D. P.; DiStasio, R. A.; Lochan, R. C.; Wang, T.; Beran, G. J. O.; Besley, N. A.; Herbert, J. M.; Lin, C. Y.; Van Voorhis, T.; Chien, S. H.; Sodt, A.; Steele, R. P.; Rassolov, V. A.; Maslen, P. E.; Korambath, P. P.; Adamson, R. D.; Austin, B.; Baker, J.; Byrd, E. F. C.; Dachsel, H.; Doerksen, R. J.; Dreuw, A.; Dunietz, B. D.; Dutoi, A. D.; Furlani, T. R.; Gwaltney, S. R.; Heyden, A.; Hirata, S.; Hsu, C. P.; Kedziora, G.; Khalliulin, R. Z.; Klunzinger, P.; Lee, A. M.; Lee, M. S.; Liang, W.; Lotan, I.; Nair, N.; Peters, B.; Proynov, E. I.; Pieniazek, P. A.; Rhee, Y. M.; Ritchie, J.; Rosta, E.; Sherrill, C. D.; Simmonett, A. C.; Subotnik, J. E.; Woodcock, H. L.; Zhang, W.; Bell, A. T.; Chakraborty, A. K.; Chipman, D. M.; Keil, F. J.; Warshel, A.; Hehre, W. J.; Schaefer, H. F.; Kong, J.; Krylov, A. I.; Gill, P. M. W.; Head-Gordon, M. *Phys. Chem. Chem. Phys.* **2006,** *8*, 3172.

5. Breneman, C.M.; Wiberg, K.B. *J. Comput. Chem.* **1990**, *11*, 361-373.

6. Peng, D.-Y.; Robinson, D. B. *Ind. Eng. Chem. Fundamen.* **1976**, *15*, 59−64.

7. Gupta, A.; Chempath, S.; Sanborn, M.J.; Clark, L.A.; Snurr, R.Q. *Mol. Simul.* **2003**, *29*, 29−46.

8. Martin, M. J.; Siepmann, J.I. *J. Phys. Chem. B* **1998**, *102*, 2569−2577.

9. Levesque, D.; Gicquel A.; Darkrim., F. L.; Kayiran S. B. *J. Phys.-Condes. Matter*, **2002**, *14*, 9285−9293.

10. Potoff, J. J.; Siepmann, J. I. *AIChE Journal* , **2002**, *47*, 1676−1682.